Thermal Styrene-*co*-Acrylonitrile Discoloration Problem: The Role of Sequence Distribution and Oligomers

D. S. Allan, M. Birchmeier, J. R. Pribish, D. B. Priddy,* and P. B. Smith

Dow Plastics, Midland, Michigan 48667

C. Hermans

Dow Plastics Europe, 4530AA Terneuzen, The Netherlands

Received June 27, 1993[⊗]

ABSTRACT: Styrene-*co*-acrylonitrile resins (SAN) are important commercial thermoplastic materials. However, SAN discolors during molding, the extent of which is dependent upon the AN content of the polymer. GPC–UV/vis analysis of discolored SAN indicates that both monomer sequence distribution in the backbone and small molecules are involved in the formation of chromophores and that the main backbone chromophore resides on the chain end. The product of reactivity ratios (calculated from monomer sequence distribution data) of high-temperature (140–160 °C), CSTR-produced SAN copolymers is higher than typically reported for low-conversion batch copolymerization. Possible mechanisms are proposed for (1) a high reactivity ratio product, (2) SAN polymer backbone discoloration, and (3) the formation of small colored molecules.

Introduction

The copolymerization of styrene (S) and acrylonitrile (AN) has been studied in much detail over the last 50 years. Styrene-*co*-acrylonitrile (SAN) resins have improved toughness as well as heat and solvent resistance properties over polystyrene and have therefore become very important commercial thermoplastics. The copolymerization of S and AN is carried out commercially utilizing three types of free-radical polymerization processes, i.e., bulk, emulsion, and suspension. However, continuous bulk polymerization in well-mixed continuous stirred tank reactors (CSTR) is the preferred process for the manufacture of SAN resins for applications requiring high optical quality. The superior color and haze of SAN made by bulk polymerization is due to the lack of emulsifiers, suspending agents, salt, and water found in the alternate processes. Bulk processes of the CSTR type[1,2] are required to eliminate copolymer composition drift (the copolymer composition vs feed composition diagram for SAN is shown in Figure 1). It has been determined that as little as a 4% drift in composition leads to haze in SAN.[3] As with polsytrene, many of the users for SAN require high optical quality. However, the introduction of AN monomer units into the polystyrene backbone has a very detrimental effect upon color stability.[4]

In comparison to polystyrene, developing an understanding of SAN degradation chemistry is very challenging. The complexity of SAN is due to the many variables that the introduction of a second monomer unit brings. Examples of copolymerization variables that have been linked to SAN optical quality include AN content,[5,6] AN sequence distribution in the polymer,[7–9] oligomer structures,[10,11] impurities in the AN monomer,[12] monomer side reactions during copolymerization,[13] the potential for copolymer composition drift,[3,14] dissolved oxygen in polymerization feed,[15] and initiator type.[16] All of these factors likely influence the optical quality of SAN and must be considered before high-quality SAN can be produced. However, compared to poly(acrylonitrile) (PAN), detailed studies aimed at elucidation of mechanisms involved in the thermal discoloration of SAN are few. This lack of attention could be due partially to

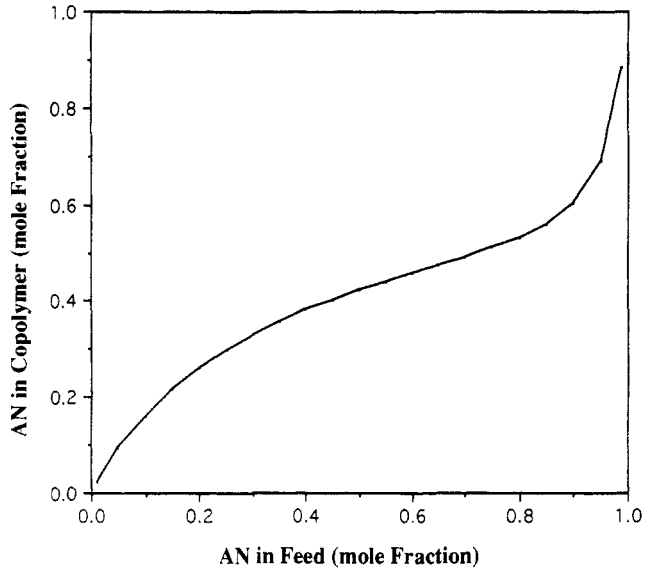

Figure 1. Feed vs. copolymer composition for the bulk copolymerization of AN and S at 130 °C. The reactivity ratios used for the calculation (terminal model) were r_A = 0.067 and r_S = 0.47.[4]

Scheme I. Cyclization of an AN Sequence to Form a Conjugated Polyimine Postulated as a Possible Mechanism of Discoloration of SAN[7]

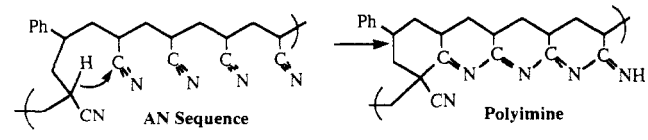

the assumption that the main mechanism of discoloration of SAN involves cyclization of AN sequences in the SAN backbone to form conjugated polyimines (Scheme I).[7] Therefore, there has been considerable interest in the development of methods for measuring AN sequence distribution in SAN and developing polymerization methods to minimize the AN sequence length.[7,8,17–25] Methods that have been developed for the determination of monomer sequence distribution in SAN include ^{13}C NMR,[26–32] infrared spectroscopy,[33–37] ultraviolet spectroscopy,[38–40] pyrolysis GC,[9,41,42] pyrolysis mass spectroscopy,[43,44] fluorescence,[45,46] GPC–IR,[17,47] and GPC–UV.[40]

[⊗] Abstract published in *Advance ACS Abstracts*, October 1, 1993.

0024-9297/93/2226-6068$04.00/0

In this study, we utilize GPC–UV/vis to analyze discolored SAN. This powerful technique has been developed recently to determine the location of chromophores in polymers[48–50] but has not yet been applied to the SAN discoloration problem. Previously, the application of GPC–UV to SAN characterization has been limited to the determination of monomer sequence distribution.[40] UV/vis by itself has been utilized to compare the discoloration of random SAN with SAN having a highly alternating structure.[7] High alternation in SAN copolymerization is achieved by the addition of an electron-deficient metal compound (e.g., $ZnCl_2$) to the polymerization. The metal forms a complex with the electron-rich nitrogen, increasing the electron-withdrawing effect of the nitrile. The result is that the Alfrey–Lewis *e*-value of AN increases.[7,8,21–23,25,51]

Experimental Section

The SAN resins used during this study were commercial TYRIL SAN resins manufactured at Dow Chemical Co. using continuous bulk polymerization in a reactor of the CSTR type at a temperature range of 150–160 °C. No chemical initiator was used. All resin samples were dried for 2 h in a circulated-air oven at 60 °C prior to molding.

Molding. The SAN resins were molded into 2.5-mm-thick plaques using an ARBURG CMD-170 injection-molding machine. The mold temperature was set at 50 °C. All resins were molded in such a way as to maintain the same residence time inside the barrel of the molding machine. As the barrel temperature of the machine was changed, the pressure was adjusted to maintain an average residence time of the resin inside the barrel of 8.5 min.

Color Measurement. The CIE Lab system[52] was used to determine color. In this system color is divided into three components, i.e., red–green (*a* component), blue–yellow (*b* component), and dark–light (*L* component). The measurements are relative and done in comparison to white and black standards. All color data shown in the figures are composite ΔE values and are calculated by

$$\Delta E = (\Delta a^2 + \Delta b^2 + \Delta L^2)^{1/2}$$

All polymer color measurements on injection-molded plaques and solutions were made using a DATACOLOR 3890 spectrophotometer.

Determination of the Contribution of Small Molecules to SAN Color. SAN resins of various AN contents were molded into plaques at low (200 °C) and at high (280 °C) temperatures. The plaques were dissolved in HPLC-grade methylene chloride (10% w/w). The color of each solution was determined using the same method described for molded plaques. The polymer was precipitated from a portion of the solution by the addition of two volumes of HPLC-grade methanol. The liquid phase was decanted and the polymer redissolved in methylene chloride. Again, two volumes of methanol were added to precipitate the polymer. This procedure was repeated a third time. The triply precipitated polymers were dried in a vacuum oven at 125 °C overnight. The dry polymers were then redissolved in methylene chloride (10% w/w) for color analysis.

AN Content and Compositional Homogeneity by HPLC. The AN content and compositional homogeneity of the SAN copolymers used during this study were measured using a HPLC method similar to that described by Gloeckner *et al.*[53] The chromatograph was a Hewlett Packard 1090M equipped with a diode array detector. The column dimensions were 4.6 × 150 mm packed with ZORBAX CN. The mobile phase was heptane/THF at a flow rate of 1 cm³/min. The column was calibrated using eight SAN copolymers having the following AN compositions: 0, 5, 15, 20, 24, 29, 37, and 48% w/w. The standards were prepared *via* CSTR polymerization. The AN contents of the copolymers were determined *via* nitrogen analysis.

GPC–UV/vis Analyses. GPC–UV/vis analyses were performed using a Hewlett Packard 1090M equipped with a diode array detector. Two 7 × 300 mm trimodal mixed-bed GPC columns, manufactured by Polymer Laboratories, were used in series. The column set was calibrated using a series of narrow polystyrene standards. UV/vis spectra (240–500 nm) were collected at a rate of 1/s during the analysis. Also, GPC signals at 260 and 400 nm (4-nm bandwidth) were recorded with a reference collected at 550 nm (50-nm bandwidth).

^{13}C NMR Analyses. The polymers were analyzed as solutions in $CDCl_3$ by ^{13}C NMR spectroscopy. The ^{13}C NMR spectra were obtained at 75.5 MHz using a Bruker AC-300 NMR spectrometer, Model HO2129-ECL-24. The data acquisition parameters utilized were as follows: pulse width = 90°, delay time = 10 s, size = 16K, accumulation time = 0.41 s, sweep width = 20 kHz, apodization = exponential, 5-Hz broadening, decoupling = gated without NOE.

Results and Discussion

The copolymerization kinetics of SAN have been the subject of numerous studies over the past 50 years. In most studies, the terminal copolymerization model has been applied to SAN copolymerization and many reactivity ratio values have been calculated according to this model. The reactivity ratios for the addition of AN and S to a growing polymer radical are r_A and r_S, respectively.

However, some investigators have observed that the terminal model is not adequate to interpret their results, and thus more sophisticated models have been evaluated. Ham[54] was the first to notice deviation of SAN copolymerization from the simple terminal model, and he explains the deviation based upon penultimate effects. Since that time several other researchers have also noticed deviations of their data from the terminal model and have applied more elaborate copolymerization models to explain the mechanism of SAN copolymerization. The penultimate and complex participation models have both been evaluated and give a better fit to the SAN system than the terminal model.[55–57] Most recently, Hill *et al.*[26,46,58,59] compared all three models and found that the penultimate model gave the best fit to their NMR sequence distribution data obtained from SAN copolymers made using bulk and solution polymerization at 60 °C.

Pichot *et al.*[60] also observed deviation from the terminal model and offered several possible explanations for these discrepancies: (1) preferential solvation of one of the monomers in the polymer; (2) AN existing as a dimer due to dipole–dipole interactions; (3) terminal radical interaction with the AN nitrile group.

Theoretically, if the terminal reactivity ratio data from the literature is of sufficient quality, Arrhenius plots would show the temperature sensitivity of the reactivity ratios and one could calculate activation energy differences for the addition of S and AN monomers to S and AN terminal growing polymer radicals, respectively (Scheme II).[14,61–63]

A plot of all of the terminal reactivity ratio data from the literature shows, even with the significant scatter (especially the r_A numbers), that r_A, r_S, and the product of r_A and r_S approach unity at infinite temperature (Figure 2). The data scatter is likely due to the large number of researchers using a variety of techniques for reactivity ratio calculation. Plotting the data of one researcher alone should solve this problem. Johnston[4] was chosen because he collected reactivity ratio data for bulk SAN copolymerization over a broad temperature range (−30 to +130 °C). Indeed, the Arrhenius plot of his data almost perfectly intersects the logarithmic axis at 0 (Figure 3).

A key problem for the use of literature reactivity ratio data for studies of SAN discoloration is that most commercial SAN resins are produced at temperatures (140–160 °C) well above the range of temperatures typically used in literature studies to determine reactivity ratio data. However, from Figure 3 the predicted reactivity ratios at

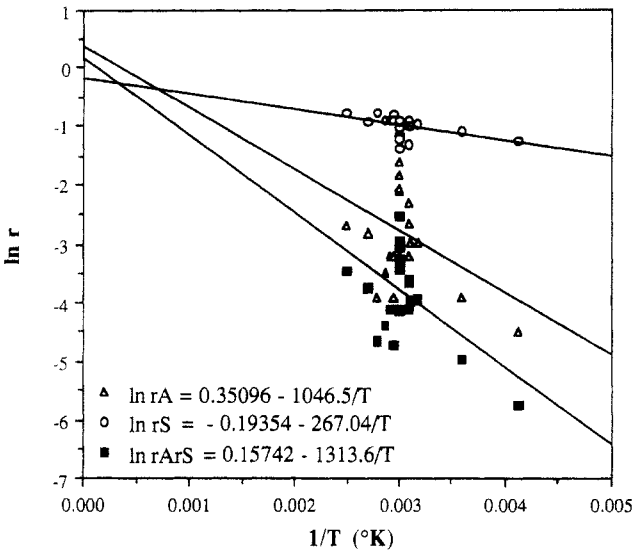

Figure 2. Arrhenius plot (least-squares fit) of the literature terminal reactivity ratio data for SAN copolymerization vs temperature.

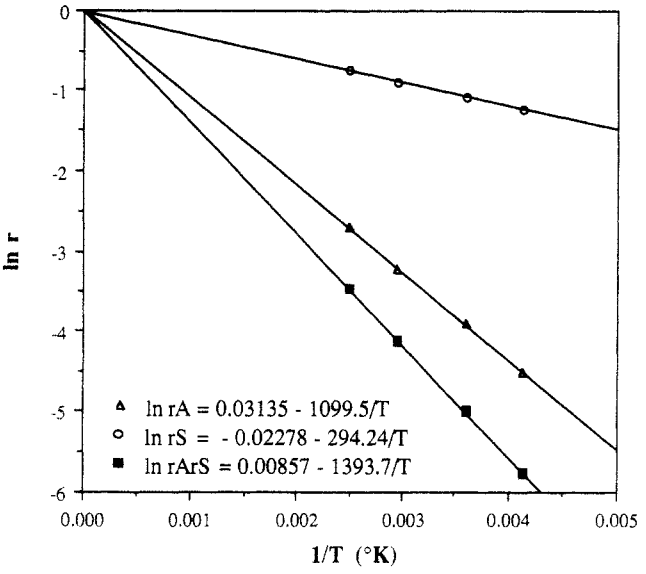

Figure 3. Arrhenius plot of Johnston's terminal reactivity ratio data for SAN copolymerization vs temperature.[4]

Scheme II. Relationship of Reactivity Ratios to Arrhenius Parameters

$$r_A = k_{AA}/k_{AS} \; ; \; r_S = k_{SS}/k_{SA}$$

$$k_{AA} = A_{AA}e^{-Ea_{AA}/RT} \qquad k_{AS} = A_{AS}e^{-Ea_{AS}/RT}$$

$$r_A = \frac{A_{AA}}{A_{AS}}\, e^{-(Ea_{AA}-Ea_{AS})/RT}$$

Assume $A_{AA} \sim A_{AS}$

$$r_A = e^{-(Ea_{AA}-Ea_{AS})/RT} \longrightarrow 1 \text{ as } T \longrightarrow \infty$$

$r_A < 1 \longrightarrow Ea_{AA} > Ea_{AS}$

$r_A > 1 \longrightarrow Ea_{AA} < Ea_{AS}$

$$\ln r_A = -[(Ea_{AA}-Ea_{AS})/R]\, 1/T$$

Slope $< 0 \longrightarrow Ea_{AA} > Ea_{AS}$

Slope $> 0 \longrightarrow Ea_{AA} < Ea_{AS}$

160 °C can be calculated from the relationships in Scheme II (r_A = 0.08 and r_S = 0.49).

Table I. AN Content of Copolymers and Their Respective Triad Distributions by ^{13}C NMR[a]

AN	SSS	SSA/ASS	ASA	SAS	AAS/SAA	AAA
0.25	0.33	0.32	0.07	0.26	0.02	
0.34	0.17	0.37	0.12	0.30	0.04	
0.39	0.11	0.34	0.16	0.32	0.07	
0.47	0.05	0.25	0.23	0.30	0.16	0.01
0.52	0.02	0.19	0.27	0.28	0.21	0.03
0.58	0.01	0.10	0.30	0.23	0.30	0.06

[a] All numbers are mole fractions, and the triad distributions are normalized to 1.0.

Another problem with literature studies is that they are typically performed using low-conversion batch polymerization. In the current study, SAN samples were prepared using a continuous bulk polymerizer of the CSTR type. The feed ratios used to prepare these resins are unknown. Triad sequence distributions (Table I) were measured using ^{13}C NMR analysis.

If the feed composition data are known, reactivity ratios can be calculated from triad compositions using the equations developed by Chujo *et al.*[64] For example, Hill *et al.*[26] calculated the terminal reactivity ratios for bulk SAN copolymerization at 60 °C to be r_A = 0.08 and r_S = 0.47 using triad sequence data.

Even though the feed compositions are not known, the product of r_A and r_S can be determined by fitting the terminal model predictions to the copolymer composition and triad data. Following the statistical deviation of the terminal copolymerization model, the mole fraction of any sequence can be expressed as a combination of the conditional probabilities for adding a certain monomer, given that the growing chain ends in a certain reactive group.

$p(A|S)$ = probability of adding A, given that the growing chain ends with an S terminal group

$$p(S|S) = 1 - p(A|S)$$

$p(S|A)$ = probability of adding S, given the growing chain ends with an A terminal group

$$p(A|A) = 1 - p(S|A)$$

The sequence distributions for which we have data are expressed in terms of the conditional probabilities in Table II.

The conditional probabilities are expressed in terms of the reactivity ratios, r_A and r_S, and the monomer feed ratio F.

$$F = [A]/[S]$$

$$p(A|S) = \left(\frac{F}{F + r_S}\right) \qquad p(S|A) = \left(\frac{1}{1 + Fr_A}\right)$$

Since the monomer feed ratio F for these experiments is unknown, it was eliminated algebraically from the expressions for the conditional probabilities to get

$$r_A r_S = 1 - \frac{1}{p(S|A)} - \frac{1}{p(A|S)} + \frac{1}{p(S|A)\, p(A|S)}$$

Thus, if the two conditional probabilities $p(S|A)$ and $p(A|S)$ can be determined accurately, then the reactivity ratio product is determined.

We determined the conditional probabilites by performing a nonlinear least-squares fit of the composition and sequence distribution data to the expressions in Table II. The values of $p(S|A)$ and $p(A|S)$ were varied to minimize the sum of the squared differences between observed and calculated sequence distributions. Each SAN sample was

Table II. Expressions for Composition and Triad Fractions in Terms of First-Order Markov Conditional Probabilities

sequence	sequence mole fraction
A (mole fraction)	$\frac{p(A\|S)}{p(A\|S) + p(S\|A)}$
AAA	$\frac{p(A\|S)}{p(A\|S) + p(S\|A)} \times p(A\|A)^2$
AAS, SAA	$2 \times \frac{p(A\|S)}{p(A\|S) + p(S\|A)} \times p(A\|A) \times p(S\|A)$
ASA	$\frac{p(A\|S)}{p(A\|S) + p(S\|A)} \times p(S\|A) \times p(A\|S)$
ASS, SSA	$2 \times \frac{p(A\|S)}{p(A\|S) + p(S\|A)} \times p(S\|A) \times p(S\|S)$
SAS	$\frac{p(S\|A)}{p(A\|S) + p(S\|A)} \times p(A\|S) \times p(S\|A)$
SSS	$\frac{p(S\|A)}{p(A\|S) + p(S\|A)} \times p(S\|S)^2$

Table III. Conditional Probabilities and $r_A r_S$ Calculated by a Nonlinear Least-Squares Fit to the Composition and Triad Data (^{13}C NMR) for the Six SAN Samples from Table I

AN	$p(S\|A)$	$p(A\|S)$	$r_A r_S$
0.25	0.98	0.33	0.04
0.34	0.94	0.47	0.007
0.39	0.90	0.54	0.09
0.47	0.79	0.67	0.13
0.52	0.73	0.75	0.12
0.58	0.62	0.86	0.10
			av = 0.09

analyzed separately, since in general each SAN had a different monomer feed ratio and therefore had different conditional probabilities. The calculated values of the reactivity ratio product ($r_A r_S$) and probabilities $p(S|A)$ and $p(A|S)$ for each of the copolymers from Table I are summarized in Table III.

The reactivity ratio products are higher than typically reported for SAN. By extrapolation of Johnston's data (Figure 3) to obtain the predicted $r_A r_S$ at 160 °C, a value of 0.0392 is obtained. The high reactivity ratio product values we obtained could be due to the way in which our SAN samples were produced compared to most academic studies. Typically, a copolymerization study is conducted using batch polymerizations which are stopped at low monomer conversion (<10%) to minimize composition drift. Thus the polymerizations are carried out at low viscosity. However, the SAN copolymers used in this study were prepared in a CSTR bulk polymerization process at high monomer conversion (>50%) Studies of homopolymerizations carried out in viscous media show that the propagation rate slows down as the viscosity increases due to the slow rate of diffusion of unreacted monomer to the radical sites. Since acrylonitrile is smaller than styrene, it would differ faster through viscous media, thus increasing r_A. This hypothesis is in line with observations by researchers studying the kinetics of polymerizations taken to high monomer conversions.[59,65,66] Thus SAN copolymers prepared in CSTR processes operating at high viscosity will have higher $r_A r_S$ values (longer AN sequences) than SAN copolymers prepared in processes operating at low viscosity. This, of course, is bad if SAN discoloration involves the cyclization of AN sequences.

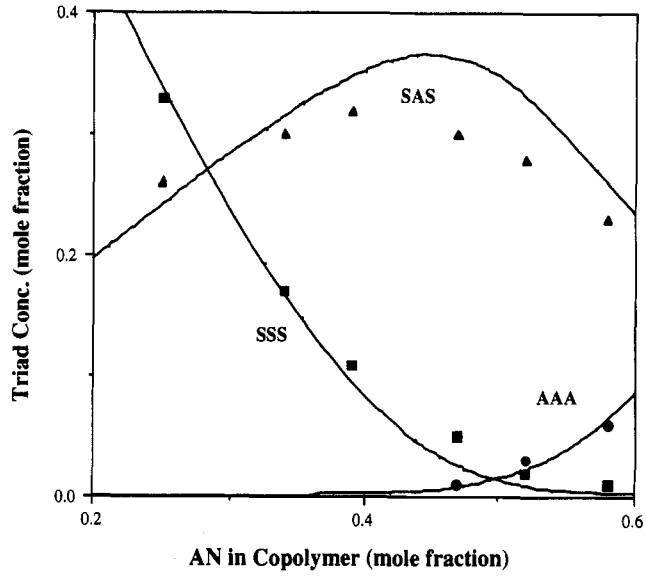

Figure 4. Overlay of the actual and calculated triads using $r_A = 0.08$ and $r_S = 0.49$.

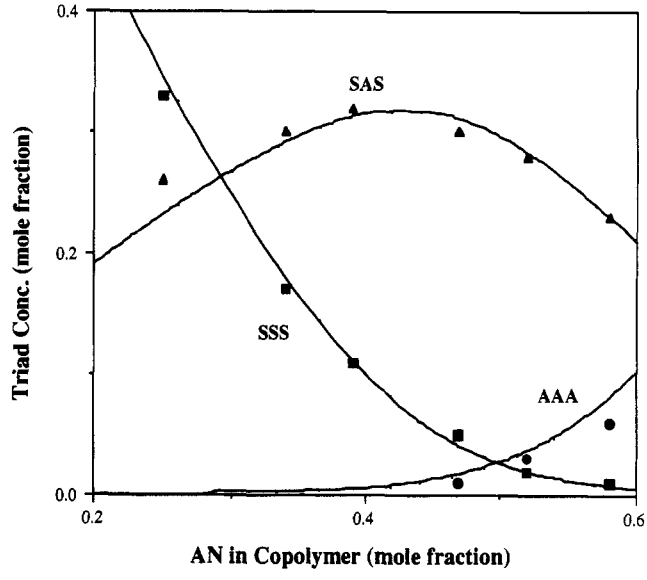

Figure 5. Overlay of the actual and calculated triads using $r_A = 0.18$ and $r_S = 0.49$.

Harwood[67] presents evidence indicating that it is the monomer concentrations local to the active radical center that control the copolymerization and backbone monomer sequence distribution rather than the average monomer concentrations in the reactor. Harwood calls this the "bootstrap model" because it is the nature of the polymer chain itself that controls the local monomer concentration near its active chain end. In a poor solvent, the relative concentration of AN inside the polymer coil could be higher than outside the coil, causing an increase in the value of r_A and the length of AN sequences.

Using the predicted reactivity ratios at 160 °C from Johnston,[4] the relationship between triad fractions and composition is plotted (Figure 4). The agreement is good for SSS and AAA triads but less so for SAS. Assuming the r_S value to be correct, better agreement is achieved by adjusting r_A upward to 0.18 (Figure 5). This adjustment gives a reactivity ratio product value of 0.09 which is the same as the average value obtained from our calculations on the SAN copolymers in Table I.

For the rest of this discussion, we will use the reactivity ratios of $r_A = 0.18$ and $r_S = 0.49$ for our high-temperature

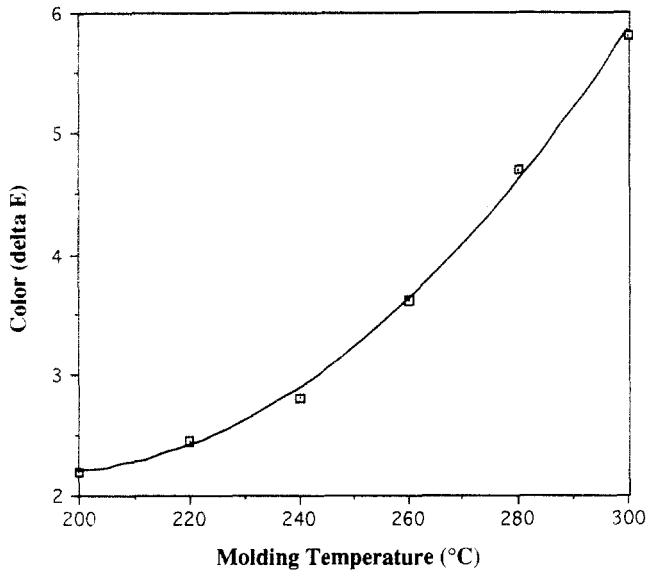

Figure 6. Increase in the color of SAN (0.433 mole fraction AN), with molding temperature.

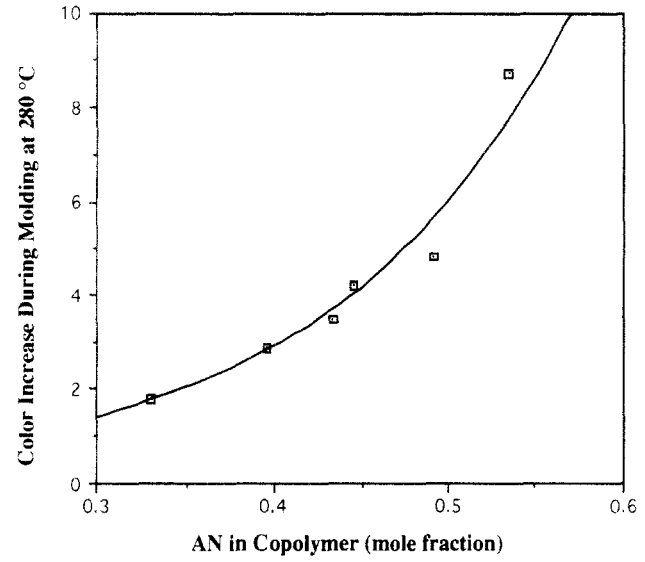

Figure 7. Increase in SAN color during molding at 280 °C as the AN content of SAN increases.

CSTR-produced SAN copolymers because they appear to better fit the sequence distribution data.

Correlation of SAN Discoloration with AN Sequence Distribution

The mole fraction range of AN found in commercial SAN resins is 0.25–0.55. When SAN is molded, it discolors. The extent of discoloration in molded plaques increases with both molding temperature (Figure 6) and AN content (Figure 7).

If the discoloration chemistry is due mainly to the cyclization of AN sequences, the increase in discoloration with increasing AN content should correspond to the increase in AN sequences. To see if a correlation exists, we calculated the AAA triads vs copolymer composition using the terminal model, with reactivity ratios of 0.18 and 0.49 for r_A and r_S, respectively. The results (Figure 8) show a good correlation between the discoloration of molded plaques and the AAA triad concentration, suggesting that AN cyclization chemistry is likely a contributor to SAN discoloration during molding.

Since the bulk discoloration of SAN may involve the formation of visible chromophores both in the polymer backbone and in the small molecules present (e.g., monomers, oligomers, impurities), we chose to utilize GPC–UV/vis to separate the contribution of the polymeric component (DP > 20) from the small molecule (DP < 20) component.

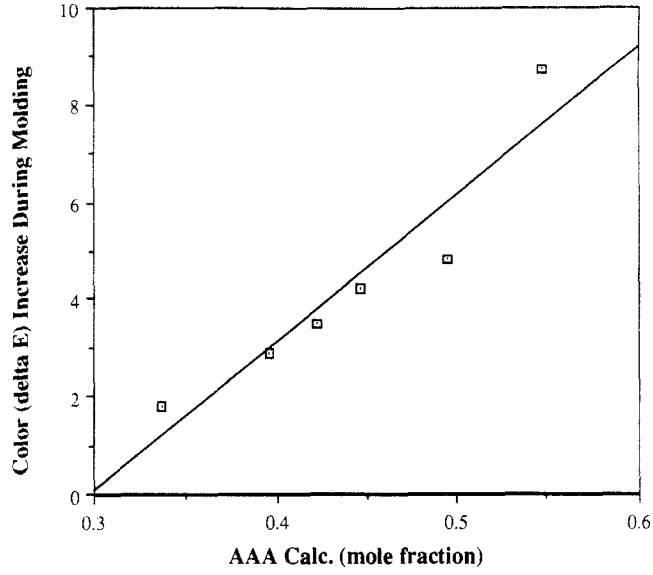

Figure 8. Color increase during molding at 280 °C vs the AN triads calculated from the terminal model using r_A = 0.18 and r_S = 0.49.

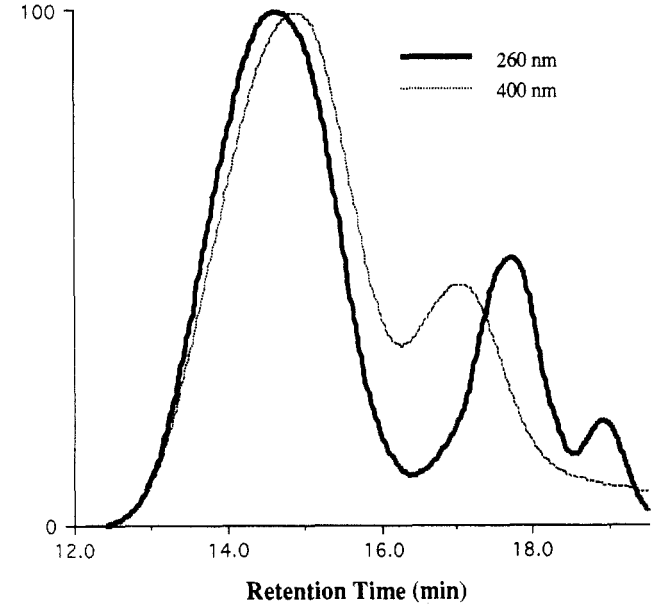

Figure 9. Overlay of the 260- and 400-nm GPC curves.

Five bulk CSTR-prepared SAN copolymers having different AN contents were thermolyzed in evacuated (<4 mmHg) glass ampules at 250 °C for 72 h and analyzed using GPC–UV/vis. Figure 9 shows an overlay of GPC curves collected simultaneously at 260 and 400 nm of the thermolyzed SAN resin (0.492 mole fraction AN). Before thermolysis, the absorptivity of the polymer at 400 mm was too small to get a signal. Figure 10 shows the 3D plot (absorbance vs wavelength vs time) of the same sample. Both the overlay of the 260- and 400-nm GPC curves (Figure 9) and the 3D view of the GPC (Figure 10) show that absorbance in the visible is present in both high and low molecular weight polymer fractions.

The area under the high molecular weight polymer portion of the 400-nm GPC curves increased with AN content (Figure 11). Excellent correlation was found between the area under the 400-nm GPC curve of the high polymer portion of five samples vs the calculated AAA

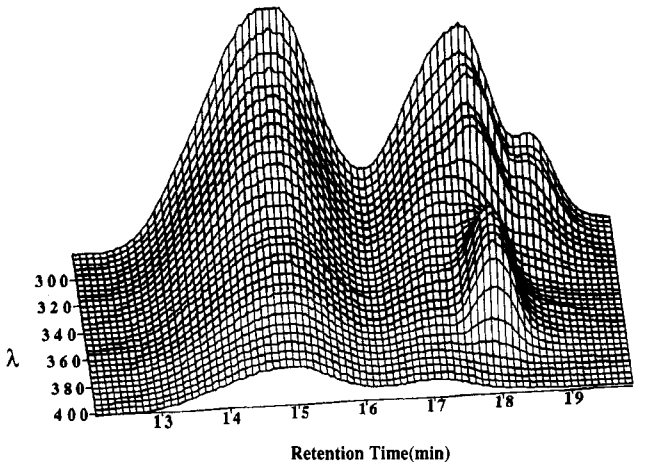

Figure 10. 3D view of GPC analysis of discolored SAN.

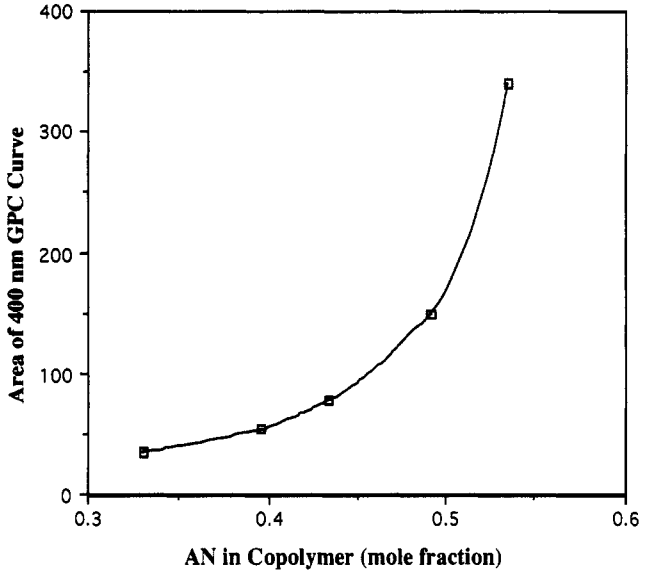

Figure 11. Area under the high polymer portion of the 400-nm GPC curve vs AN content.

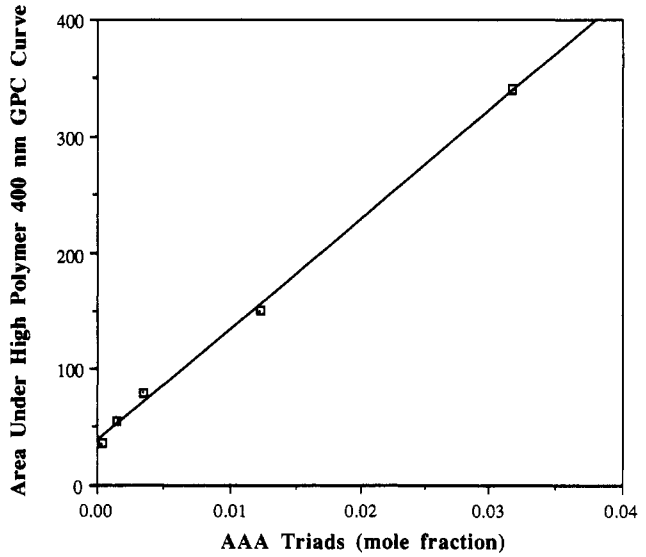

Figure 12. Area of the high polymer portion of the 400-nm GPC curve of discolored SAN vs AAA triad concentration calculated using $r_A = 0.18$ and $r_S = 0.49$.

triad content of the copolymers (Figure 12). The correlation of color in the high polymer with AAA triads (Figure 12) is better than the correlation of bulk discoloration with AAA triads (Figure 8). This suggests that there is

Scheme III. Possible Mechanism of Chain-End Chromophore Formation in SAN Consistent with GPC-UV/Vis Data and the Inhibiting Effect of Hindered Phenol Antioxidants

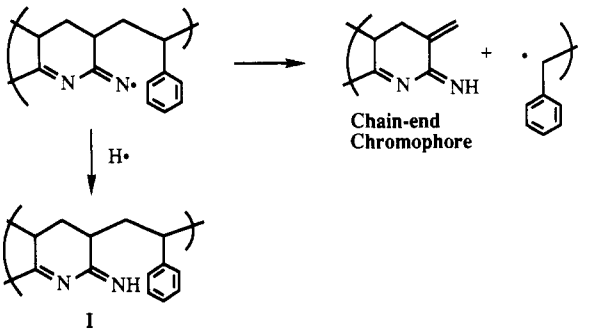

I

a significant contribution of color in the small molecules to the overall bulk discoloration.

The chromophore in the high polymer portion appears to be located primarily on the chain ends as evidenced by an offset of the 400-nm GPC curve to the low molecular weight side of the 260-nm GPC curve (Figure 9). This offset occurs because the concentration of end-group chromophores absorbing at 400 nm relative to random backbone chromophores absorbing at 260 nm increases as chain length decreases. A thorough discussion of this phenomenon is presented elsewhere.[48-50] This finding indicates that the chain-end chromophore mechanism of discoloration proposed by Grassie and McGuchan (Scheme III)[68] may be operative. The reported observation that the addition of hindered phenol antioxidants improves color stability[69] also supports the Grassie mechanism since the hindered phenol would quench the terminal iminyl radical (**I**) before chain scission and subsequent chromophore formation takes place (Scheme III).

A key consideration is the potential for discoloration chemistry of small molecules (monomers and oligomers) to be much different than that of the polymer, since the oligomers cannot contain long AN sequences. Thus we decided to determine the relative contribution of small molecules and high polymer to SAN bulk discoloration during molding. To determine this, we molded two SAN resins (0.395 and 0.492 mole fraction AN) at low (200 °C) and high (280 °C) temperature. The molded plaques were dissolved (10% w/w) in methylene chloride, and the color of the solutions measured. Then the high polymer fraction was precipitated (pct) by the addition of two parts of methanol. The pct polymers were dried in a vacuum oven at 60 °C and redissolved in methylene chloride, and the color was remeasured. About half of the discoloration was found to be due to small (methanol-soluble) molecules (Figure 13).

There is a strong increase in the UV absorbance between 340 and 360 nm of oligomers in the 2–3 DP range (Figure 10). Overlay of the UV spectrum collected in this region with the UV spectrum of 2-amino-3-methyl-1-naphthalenecarbonitrile (AMNC)[70] confirms that the increase in absorbance between 340 and 360 nm is due to the decomposition of one of the SAN trimers [4-cyano-1,2,3,4-tetrahydromethyl-1-naphthaleneacetonitrile (CTMN)] containing one styrene and two acrylonitrile units as shown in Scheme IV.[71] CTMN is a byproduct of the spontaneous initiation mechanism of SAN.[70,72]

Discoloration Chemistry of Oligomers

The chemistry involved in the formation of the methanol-soluble colored molecules in SAN is not clear. AMNC crystals are only very slightly yellow. In fact, AMNC was

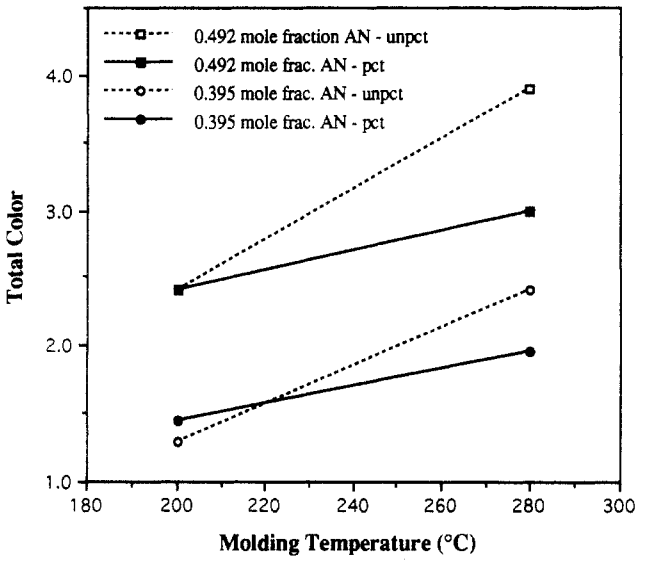

Figure 13. Color of two (pct and unpct) SAN resins (0.395 and 0.492 mole fraction AN) molded at low and high temperatures.

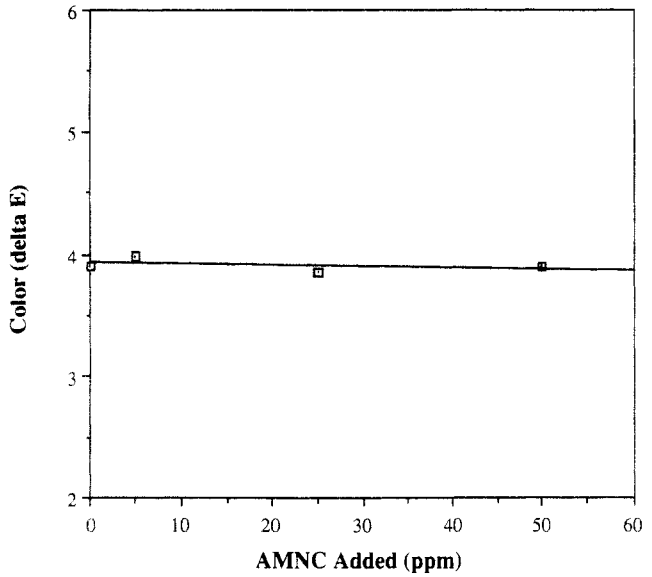

Figure 14. Contribution of AMNC to the color (ΔE) of SAN in solution.

Scheme IV. Rearrangement of a SAN Trimer upon Heating To Form a Naphthalene Derivative Having Strong UV Absorbance between 340 and 360 nm

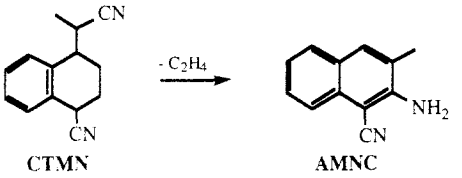

spiked at concentrations up to 50 ppm into a methylene chloride solution of SAN with no affect on color (Figure 14).

However, it is possible that AMNC is involved in the formation of chromophores in low molecular weight species. For example, CTMN fragments are likely attached to some short chains *via* the spontaneous initiation mechanism. If the CTMN fragments undergo rearrangement to AMNC fragments, the result could be molecules having enough conjugation to absorb >400 nm.

Another possible mechanism for AMNC to become involved in the formation of molecules that absorb at >400 nm is by condensation of its amino group with carbonyl-containing impurities in the polymer. For example, most styrenic polymers contain traces of benzaldehyde. Indeed, we found that heating AMNC with benzaldehyde forms intensely yellow mixtures.

Conclusions and Recommendations

The results of this investigation show that the discoloration chemistry of SAN is complex and not limited to one factor or mechanism. Both the monomer unit sequence distribution and small-molecule residues in the polymer contribute about equally to the overall bulk discoloration during molding. The SAN backbone chromophores appear to be located primarily on the chain ends, and a radical chain-scission mechanism involving nitrile cyclization is proposed which is consistent with the stabilizing effect of hindered phenol antioxidants observed by other researchers.

The mechanism of formation of chromophores in the oligomeric fraction of the polymer is uncertain. It is possible that oligomers decompose to form chromophores or that the polymer unzips, slitting off colored oligomers from the high polymer.

Since it appears that the formation of chromophores in the polymer backbone involves the cyclization of AN sequences, the color stability of SAN should be improved by increasing the alternation tendency of the polymerization. This can be accomplished by conducting the polymerization to minimize the value r_A. The value of r_A can be decreased by polymerizing at lower temperature, adding Lewis acid to the feed, or possibly decreasing the viscosity of the polymerizing mass.

References and Notes

(1) Hanson, A. W.; Zimmerman, R. L. *Ind. Eng. Chem.* **1957**, *49*, 1803.
(2) Hanson, A. W.; Best, J. S. U.S. Patent 2989517, 1961.
(3) Molau, G. E. *J. Polym. Sci., Part B* **1965**, *3*, 1007.
(4) Johnston, N. W. *J. Macromol. Sci., Rev. Macromol. Chem.* **1976**, *C14*, 215.
(5) Illig, S. A. *SPE ANTEC* **1989**, 876.
(6) Illig, S. A. *Rev. Plast. Mod.* **1990**, *60*, 409.
(7) Yabumoto, S.; Ishii, K.; Kawamori, M.; Arita, K.; Yano, H. *J. Polym. Sci., Part A* **1969**, *7*, 1683.
(8) Yabumoto, S.; Ishii, K.; Arita, K. *J. Polym. Sci., Part A* **1969**, *7*, 1577.
(9) Yamamoto, Y.; Tsuge, S.; Takeuchi, T. *Kobunshi Kagaku* **1972**, *29*, 407.
(10) Schellenberg, J.; Hamann, B. *Angew. Makromol. Chem.* **1991**, *187*, 123.
(11) Schellenberg, J.; Wigand, G. *Makromol. Chem.* **1992**, *193*, 3063.
(12) Wild, H.; Jung, R.; Echte, A.; Zizisperger, J.; Gausepohl, H. U.S. Patent 4061858, 1977.
(13) Patron, L.; Bastianelli, U. *Appl. Polym. Symp.* **1974**, *25*, 105.
(14) Tirrell, M.; Gromley, K. *Chem. Eng. Sci.* **1981**, *36*, 367.
(15) Kent, R. W. U.S. Patent 4,243,781, 1981.
(16) Kent, R. W. U.S. Patent 4,268,652, 1981.
(17) Mori, S.; Wada, A.; Kaneuchi, F.; Ikeda, A.; Watanabe, M.; Mochizuki, K. *J. Chromatogr.* **1982**, *246*, 215.
(18) Yabumoto, S.; Ishii, K.; Arita, K. *J. Polym. Sci., Polym. Chem. Ed.* **1970**, *8*, 295.
(19) Patnaik, B. K.; Takahashi, A.; Gaylord, N. G. *J. Macromol. Sci., Chem.* **1970**, *4*, 143.
(20) Gaylord, N. G.; Patnaik, B. *J. Polym. Sci., Part B* **1970**, *8*, 401.
(21) Gaylord, N. G.; Dixit, S. S.; *J. Polym. Sci., Part B* **1971**, *9*, 823.
(22) Gaylord, N. G.; Dixit, S. S.; Maiti, S.; Patnaik, B. K. *J. Macromol. Sci., Chem.* **1972**, *6*, 1495.
(23) Gaylord, N. G. U.S. Patent 3919182, 1975.
(24) Gaylord, N. G.; Tomono, T. *J. Polym. Sci., Polym. Lett. Ed.* **1975**, *13*, 697.
(25) Schaefer, J. *Macromolecules* **1971**, *4*, 107.
(26) Hill, D. J. T.; O'Donnell, J. H.; O'Sullivan, P. W. *Macromolecules* **1982**, *15*, 960.
(27) Stejskal, E. O.; Schaefer, J. *Macromolecules* **1974**, *7*, 14.
(28) Sandner, B.; Keller, F.; Roth, H. *Faserforsch. Textiltech.* **1975**, *26*, 278.
(29) Pichot, C.; Pham, Q. T. *Makromol. Chem.* **1979**, *180*, 2359.

(30) Arita, K.; Ohtomo, T.; Tsurumi, Y. *J. Polym. Sci., Polym. Lett. Ed.* **1981**, *19*, 211.
(31) Barron, P. F.; Hill, D. J. T.; O'Donnell, J. H.; O'Sullivan, P. W. *Macromolecules* **1984**, *17*, 1967.
(32) Keller, F.; Sandner, B. *Faserforsch. Textiltech.* **1976**, *27*, 45.
(33) Sargent, M.; Koenig, J. L.; Maecker, N. L. *Appl. Spectrosc.* **1991**, *45*, 1726.
(34) Oi, N.; Moriguchi, K. *Bunseki Kagaku* **1974**, *23*, 798.
(35) Littke, W. H.; Fieber, W.; Schmolke, R.; Kimmer, W. *Faserforsch. Textiltech.* **1975**, *26*, 503.
(36) Nyquist, R. A. *Appl. Spectrosc.* **1987**, *41*, 797.
(37) Wolfram, L. E.; Grasselli, J. G.; Koenig, J. L. *Appl. Polym. Symp.* **1974**, *25*, 27.
(38) Garcia, R. L. H.; Ro, N. *Can. J. Chem.* **1985**, *63*, 253.
(39) Bruessau, R. J.; Stein, D. J. *Angew. Makromol. Chem.* **1970**, *12*, 59.
(40) Garcia, R. L. H.; Hamielec, A. E.; MacGregor, J. F. *ACS Symp. Ser.* **1982**, *197*, 151.
(41) Blazso, M.; Varhegyi, G.; Jakab, E. *J. Anal. Appl. Pyrolysis* **1980**, *2*, 177.
(42) Nagaya, T.; Sugimura, Y.; Tsuge, S. *Macromolecules* **1980**, *13*, 353.
(43) Tsuge, S.; Kobayashi, T.; Sugimura, Y.; Nagaya, T.; Takeuchi, T. *Macromolecules* **1979**, *12*, 988.
(44) Tsuge, S.; Sugimura, Y.; Kobayashi, T.; Nagaya, T. *Polym. Prepr. (Am. Chem. Soc., Div. Polym. Chem.)* **1981**, *22*, 284.
(45) Alexandru, L.; Somersall, A. C. *J. Polym. Sci., Polym. Chem. Ed.* **1977**, *15*, 2013.
(46) Hill, D. J. T.; Lewis, D. A.; O'Donnell, J. H.; O'Sullivan, P. W.; Pomery, P. J. *Eur. Polym. J.* **1982**, *18*, 75.
(47) Bartick, E. G. *J. Chromatogr. Sci.* **1979**, *17*, 336.
(48) Warner, S. L.; Howell, B. A.; Smith, P. B.; Dais, V. A.; Priddy, D. B. *J. Appl. Polym. Sci.* **1992**, *45*, 461.
(49) Priddy, D. B.; Mork, C. O.; Warner, S. L.; Dais, V. A. *SPE ANTEC Proc.* **1992**, 1166.
(50) Mork, C. O.; Priddy, D. B. *J. Appl. Polym. Sci.* **1992**, *45*, 435.
(51) Seymour, R. B.; Stahl, G. A.; Garner, D. P.; Knapp, R. D. *Polym. Prepr. (Am. Chem. Soc., Div. Polym. Chem.)* **1976**, *17*, 216.
(52) Billmeyer, F. W.; Saltzman, M. *Principles of Color Technology*; John Wiley & Sons: New York, 1981.
(53) Gloeckner, G.; Van den Berg, J. H. M. *Chromatographia* **1987**, *24*, 233.
(54) Ham, G. E. *J. Polym. Sci.* **1954**, *14*, 87.
(55) Hill, D. J. T.; O'Donnell, J. J.; O'Sullivan, P. W. *Prog. Polym. Sci.* **1982**, *8*, 215.
(56) Sandner, B.; Loth, E. *Faserforsch. Textiltech.* **1976**, *27*, 571.
(57) Sandner, B.; Loth, E. *Faserforsch. Textiltech.* **1976**, *12*, 633.
(58) Hill, D. J. T.; Lang, A. P.; O'Donnell, J. H.; O'Sullivan, P. W. *Eur. Polym. J.* **1989**, *25*, 911.
(59) Hill, D. J. T.; Lang, A. P.; O'Donnell, J. H. *Eur. Polym. J.* **1991**, *27*, 765.
(60) Pichot, C.; Zaganiaris, E.; Guyot, A. *J. Polym. Sci., Polym. Symp.* **1975**, *52*, 55.
(61) O'Driscoll, K. F. **1969**, *J. Macromol. Sci., Chem. A3*, 307.
(62) Balaraman, K. S.; Nadkarni, V. M.; Mashelkar, R. A. *Chem. Eng. Sci.* **1986**, *41*, 1357.
(63) Goldfinger, G.; Steidlitz, M. *J. Polym. Sci.* **1948**, *3*, 786.
(64) Chujo, K.; Harada, Y.; Tokahara, S.; Tanaka, K. *J. Polym. Sci., Part C* **1966**, *27*, 321.
(65) Sharma, D. K.; Soane, D. S. *Macromolecules* **1988**, *21*, 700.
(66) Dionisio, J. M.; O'Driscoll, K. F. *J. Polym. Sci., Polym. Lett.* **1979**, *17*, 701.
(67) Harwood, H. J. *Makromol. Chem., Macromol. Symp.* **1987**, *10/11*, 331.
(68) Grassie, N.; McGuchan, R. *Eur. Polym. J.* **1972**, *8*, 243.
(69) Vukovic, R.; Kuresevic, V.; Gnjatovic, V. *Hem. Ind.* **1974**, *28*, 565.
(70) Hasha, D. L.; Priddy, D. B.; Rudolf, P. R.; Stark, E. J.; De Pooter, M.; Van Damme, F. *Macromolecules* **1992**, *25*, 3046.
(71) Stark, E.; Bell, B. M.; Hasha, D. L.; Priddy, D. B.; Skelly, N. E.; Yurga, L. J. *J. Macromol. Sci., Macromol. Rep.* **1992**, *A29*, 1.
(72) Kirchner, K.; Schlapkohl, H. *Makromol. Chem.* **1976**, *177*, 2031.